CHAPTER VI
DEVELOPMENT OF SILK FIBROIN FILMS AS ANTIMICROBIAL WOUND DRESSINGS

6.1 Abstract

Novel antibacterial silk fibroin (SF) films have been prepared from a 5 wt.-% SF solution that contained silver nitrate ($AgNO_3$) at different concentrations (0.5, 1.0, 1.5, 2.0 and 2.5 wt.-%) by a solvent-casting technique. The $AgNO_3$-containing SF solution was aged under mechanical stirring for various time intervals to allow for the formation of silver nanoparticles (nAgs). The formation of nAgs was confirmed by using a UV-vis spectrophotometer. The morphology and size of the nAgs were characterized by transmission electron microscopy (TEM).To improve the water resistance, nAg-loaded SF films were treated with 90 vol.-% of methanol. These films were tested for their *in vitro* degradation behavior, release characteristic of the as-loaded silver, and antimicrobial activity for microorganisms. With an increase in the $AgNO_3$ content, the cumulative amount of silver released was found to increase. Finally, these films could inhibit the growth of the tested pathogens, which confirmed their applicability as antibacterial wound dressings.

(**Key-words**: Silk fibroin films; Silver nanoparticles; Antimicrobial activity)

6.2 Introduction

Dressings play a major role in modern management of certain types of open wounds (e.g., traumatic, thermal, or chronic wounds), since the moist, warm and nutritious environment of wound beds provides an ideal condition for microbial growth (Wright *et al.*, 2002; Jones *et al.*, 2004; Gallant-Behm *et al.*, 2005; Leaper, 2006). Bacterial colonization and subsequent infection can interfere with the wound healing process by producing various substances (e.g., toxins, proteases and proinflammatory molecules) which may cause an excessive and prolonged

inflammatory response of the host tissues. Ideal antimicrobial dressings should have a number of key attributes, including provision of a moist environment to enhance healing (Field and Kerstein, 1994), and broad-spectrum antimicrobial activity, including activity against antibiotic-resistant bacteria [e.g., methicillin-resistant Staphylococcus aureus (MRSA)]. A recent resurgence of the use of silver-based dressings has been ascribed to their broad spectrum antibacterial activity, as well as to a lesser possibility for inducing bacterial resistance than antibiotics.

In fact, it is well known that silver or silver ions have strong inhibitory and bactericidal effects as well as a broad spectrum of antimicrobial activity (Uchida, 1995), as it binds to tissue proteins and brings structural changes in the bacterial cell wall and nuclear membrane leading to cell distortion and death. In addition, silver nanoparticles (nAgs) have higher antimicrobial activity than bulk silver metal because nAg has a high specific surface area and a high fraction of surface atoms. The conventional method to prepare nAg involves the reduction of silver salt solution by various reducing reagents in the presence of a stabilizer. The chemicals including sodium borohydride, hydrazine, hydrogen peroxide, sodium citrate, ascorbic acid and formaldehyde are mostly used as reducing agents (Sondi *et al.*, 2003; Velikov *et al.*, 2003; Chou and Lai, 2004; Kim *et al.*, 2004; Khanna *et al.*, 2005; Lee and Tsao, 2006). However, such reducing agents involve tedious multiple step reactions and the use of organic compounds. Therefore, many green approaches have been investigated to the reduction of Ag^+ into its metallic form by the polymer consisting of different hydroxyl or amine groups that can interact with the Ag^+ cations directly, which may lead to the complexation of Ag^+ to such groups (Frattini *et al.*, 2005; Huang *et al.*, 2006; Rattanaruengsrikul *et al.*, 2009).

Among the various natural polymeric materials, silk has attracted great attention due to its natural abundance and inherent biodegradability in physiological environments. In general, *Bombyx mori* silk cocoon, from the cocoon of the domesticated mulberry silkworm, is composed of a fibrous protein fibroin core (72-81%) and a surrounding glue protein, sericin (19-28%) (Gamo *et al.*, 1977; Takasu *et al.*, 2002). Silk fibroin (SF) possesses biocompatibility (Wuand and Tian, 1996), good oxygen and water vapor permeability (Minoura *et al.*, 1990; Minoura *et al.*, 1990), minimal inflammatory reaction (Altman *et al.*, 2003), slow degradation

(Altman *et al.*, 2002), and supporting human limbal epithelial stem cell attachment and proliferation (Chirila *et al.*, 2008). Owing to the excellent properties, SF was widely used for biomedical applications, for example as an enzyme-immobilization material, as an oral dosage form (Hanawa *et al.*, 1995) and particularly as a wound dressing (Minoura *et al.*, 1990). Despite the effective properties of SF for a wound dressing, there are still some drawbacks with respect to its poor antibacterial properties. To mitigate this, nAgs can be incorporated into SF. The SF spun have been coated with nAgs by (1) simply immersing the fibers in a warm aqueous solution of the nanoparticles or (2) the tyrosine mediated reduction of Ag(I) to Ag(0) under basic conditions, or (3) the photochemical reduction of Ag(I) to Ag(0) (under irradiation with UV light) (Hardy and Scheibel, 2010). However, these coated nAgs (untrapped form) on the surface of SF could release rapidly from the matrix. Form the viewpoint of wound dressing, patient compliance and antibacterial activity would be maximized by the development of long-term sustained silver release.

Here, we report the preparation of nAg-loaded SF films to be used as antibacterial wound dressings through a simple aging $AgNO_3$-containing SF solution and casting. The incorporation of nAgs into SF matrix could provide both higher concentration of nAg loading and better controlled and sustained release characteristic of the as-loaded silver. The nAgs were generated by in situ reduction of a SF solution at room temperature without any reducing agent. Methanol was used to improve the stability of the films in a moist environment. The effect of the initial $AgNO_3$ contents on the formation of nAgs in the SF solution, release characteristics of the as-loaded silver, as well as for the antibacterial of nAg-loaded SF films activity against some common bacteria found on burn wounds were evaluated.

6.3 Experimental

6.3.1 Materials

Cocoon from *B. mori* silk worm for the preparation of silk fibroin (SF) was purchased from Phetchabun, Thailand. Silver nitrate ($AgNO_3$; 99.998 % purity) was purchased from Fisher Scientific (USA). Sodium carbonate was purchased from Mallinckrodt Chemicals (USA). All other chemicals were of

analytical reagent grade and used without further purification.

6.3.2 Sample Preparation

6.3.2.1 Preparation of nAg-Containing Silk Fibroin Solutions

A cocoon was degummed three times with 0.5 wt.-% Na_2CO_3 solution at 95 °C for 30 min to completely eliminate sericin from the fibroin fiber. Thereafter, degummed silk was washed thoroughly several times in hot distilled water and then dried in an oven at 40 °C overnight. Degummed silk as SF fiber at 10 w/v% was dissolved in mixed solvent system of $CaCl_2$: ethanol : H_2O (1 : 2 : 8 in molar ratio) at 78 °C for 1 h to obtain a regenerated SF solution. The regenerated SF solution was subsequently purified by placing into a dialysis bag with a 45 kDa molecular weight cutoff (Cellu Sep T4) and dialyzed against distilled water. The water medium was changed daily for 4 days at room temperature. The obtained SF solution was lyophilized at -40 °C and then freeze-dried to obtain the regenerated SF sponges.

The regenerated SF sponge (5 wt.-%) was dissolved in distilled water under mechanical stirring for 2 h. Silver nitrate ($AgNO_3$) at various contents (0.5, 1.0, 1.5, 2.0 and 2.5 by weight of the dry SF powder) was added and continuously stirred for a proper time interval various times to allow the formation of nAgs within these solutions.

6.3.2.2 Preparation of nAg-Loaded Silk Fibroin Hydrogel Pads

The nAg-containing SF solutions (30 ml) that had been loaded with different $AgNO_3$ concentrations were cast on a polystyrene petri dish (85 mm in diameter), followed by air-drying at room temperature for 72 h to allow the solidification. Thereafter, the nAg-loaded SF films were treated with 90 vol.-% of methanol aqueous solution for 10 min to induce SF β-sheet induction. Then, the obtained SF films were air-dried for 1 h. The thickness of the films in their dry state was about 200-240 μm.

6.3.3 Characterization

6.3.3.1 Formation of nAgs

The formation of nAg in the $AgNO_3$-containing SF solutions

that had been aged for various time intervals was confirmed by monitoring the appearance of the surface plasmon band using a Shimadzu UV-2550 UV-visible spectrophotometer. The size of the as-formed nAg along with its distribution was characterized by a JEOL JEM-2100 transmission electron microscope (TEM).

6.3.3.2 Preparation of Simulated Body Fluid Buffer

Simulated body fluid buffer has ion concentrations nearly equal to those of human blood plasma and is buffered at pH 7.40. To prepare 1000 ml of the simulated body fluid buffer, 7.996 g of sodium chloride (NaCl) was dissolved in ~500 ml of distilled water. Reagents (i.e 0.350 g of sodium hydrogen carbonate, 0.224 g of potassium chloride, 0.228 g of dipotassium hydrogen phosphate, 0.305 g of magnesium chloride, 40 ml of hydrochloric acid, 0.278 g of calcium chloride, 0.071 g of sodium sulfate, 6.057 g of tris (hydroxymethyl)aminomethane were added into previous solution one by one after the former reagent was completely dissolved. The temperature of the obtained solution was adjusted at 36.5 ℃ with a water bath, and pH of this solution was adjusted at pH 7.40 by stirring the solution and titrating 1N-HCl solution. Finally, the total volume of the solution to 1000 ml was adjusted by adding distilled water.

6.3.3.3 In Vitro Degradation Test

Protease XIV enzyme (from *Streptomyces griseus*, cat#P5147, Sigma, MO) was used in this experiment to study enzymatic degradation of SF films (Horan *et al.*, 2005). Enzyme solution was prepared at concentration of dissolved 1.0 mg/ml in simulated body fluid buffer solution (SBF, pH 7.4) which has ion concentrations nearly equal to those of human blood plasma (Lin *et al.*, 2008). The nAg-loaded SF films that had been prepared from the SF solution containing $AgNO_3$ at 2.5 wt.-% in their dry state were cut into circular discs (15 mm in diameter) and weighed in order to ascertain the initial dry weight (W_i). Thereafter, the samples were immersed in 2 ml of both SBF and the enzyme solution (SBF with enzyme) and then incubated at 37 °C for various time intervals (1, 2, 3, 4, 5, 6 and 7 d). The enzyme solutions were changed daily because protease might be less effective after 1 d. At each time, the samples were taken out from media and were then dried in an oven until of a constant weight to obtain the final weight (dry) after

specified days of incubation (W_d). The percentage of remaining weight of the nAg-loaded SF films was calculated as follows:

$$remaining\ weight\ (\%) = \frac{W_d}{W_i} \times 100 \quad (1)$$

6.3.3.4 Release Characteristics of Silver

First, the actual amount of nAg in the SF films was determined. The quantification was carried out by dissolving the films untreated with methanol in 5 ml of 95 % nitric acid (HNO_3), followed by the addition of SBF (pH 7.4) to attain a total volume of 50 ml. The actual amount of nAg within the films was then quantified by a Varian SpectrAA-300 atomic absorption spectroscope (AAS). In the release assay, disc samples of the nAg-loaded SF films that had been prepared from the SF solutions containing various $AgNO_3$ contents in their dry state were placed in 50 ml SBF for various time intervals (i.e., 1, 3, 6, 12, 24, 72, 120, 168 and 216 h). At each time point, the medium was totally removed and an equal amount of the fresh medium was replaced. The amount of the released nAg in the withdrawn medium (i.e., sample solution) was determined by AAS.

6.3.3.5 Antimicrobial Activity Assay

6.3.3.5.1 Microorganism Strains

Six bacterial strains used were *Pseudomonas aeruginosa* ATCC 27853, *Staphylococcus aureus* ATCC 25923, *Methicillin-resistant Staphylococcus aureus* DMST 20654, *Staphylococcus epidermidis* ATCC 12228, *Streptococcus agalactiae* DMST 17129, *Streptococcus pyogenes* and one fungal strain, *Candida albicans* ATCC 10231. All of these were human pathogenic microorganisms and kindly supported by National Institute of Health, Department of Medical Sciences, Ministry of Public Health, Thailand and Department of Biotechnology, Faculty of Science, Ramkhamhaeng University.

6.3.3.5.2 Agar Dilution Method

The minimal inhibition concentration (MIC) values of $AgNO_3$ were determined by an agar dilution method (Barry, 1976; National Committee for Clinical Laboratory Standards, 1990) against the microorganism strains that were usually the causative agents on the skin wound. The two-fold serial dilutions of $AgNO_3$ were mixed with the sterilized Muller-Hinton broth and agar to

the final volume of 5 ml with the final concentration from 10 mg/ml to 0.6 μg/ml and immediately poured into petri dishes (50 mm in diameter). Ten microliters of 10^4 CFU/ml of each strain were spotted and inoculated onto the plates. The plates were then incubated at 37 °C for 24 h. The inhibition of the microbial growth was compared with the growth in the control plate. After 24 h of incubation, the MIC was defined as the lowest concentration of $AgNO_3$ inhibiting the visible growth of each organism on the agar plate and the MIC measurement was done in triplicate to confirm the value of MIC for each strain.

6.3.3.5.3 Effects of The nAg Containing Silk Fibroin Solutions on Microbial Growth

The antimicrobial activity of the nAg containing SF solutions at various $AgNO_3$ concentrations was investigated (Qiu *et al.*, 2003). Each of activated microbial strains in Luria-Bertani broth at 10^8 CFU/ml concentration was seeded in a 96-well tissue-culture polystyrene plate (TCPS; Biokom Systems, Poland) and then inoculated at 37 °C under shaking until the optical density (OD) at 600 nm equal to 0.1. Each of the sterilized sample solutions (30 μl) was added into wells containing microbial culture in LB broth. For the control, 30 μl of the sterilized LB broth was added instead of the sterilized sample solutions. The tested solutions containing microorganisms were immediately measured the optical density at 600 nm and incubated 37 °C under shaking. These solutions were taken to measure the optical density at 600 nm every hour (1-8 h). The optical density was calculated to the percentage of relative viability of microorganisms as followed:

$$\textit{relative viability of microorganisms}\ (\%) = \frac{OD_{sample}}{OD_{control}} \times 100 \qquad (2)$$

6.3.3.5.4 Agar Disc Diffusion Method

The US Clinical and Laboratory Standards Institute (CLSI) disk diffusion method was used to assess the antimicrobial activity of the nAg-loaded SF films (Bauer *et al.*, 1966; Alzoreky and Nakahara, 2003). The neat SF film was used as the control. The 18 h microbial culture in Muller-Hinton broth was diluted to approximately 10^5 CFU/ml with 0.85 %w/v normal saline solution. The microbial solutions were spread over the Muller-Hinton agar plates. The tested films

were cut into circular discs with 15 mm diameter and sterilized with 70 vol.-% ethanol aqueous solution for 30 min. Furthermore, all samples were placed on microorganisms-cultured agar plates and incubated at 37 °C for 24 h. The inhibition zone was monitored and the mean value was calculated.

6.3.3.6 Statistical Analysis

Data were presented as means ± standard errors of means (n = 3). A one-way ANOVA was used to compare the means of different data sets, and equal variances assumed using Scheffé's method. The statistical significance was accepted at a 0.05 confidence level.

6.4 Results and Discussion

6.4.1 Formation of nAgs in $AgNO_3$-Containing Silk Fibroin Solutions

In the present study, a SF solution at concentration of 5 wt.-% that contained $AgNO_3$ was prepared. nAgs were subsequently formed in the $AgNO_3$-containing SF solution after it had been aged for various time intervals. The formation of nAgs in the $AgNO_3$-containing SF solution after it had been aged for various time intervals can be identified simply by a change in the color of the solution from light yellow to dark brown with increasing the aging time and by a change in the UV-vis absorption spectrum.

Figure 6.1 shows spectrophotometric evidence for the formation of nAgs. It has been shown in the literature that the formation of nAgs can be observed from the appearance of the surface plasmon resonance absorption peak that centers around 416–445 nm in the UV spectrum, with the peak position hypothetically decreasing with a decrease in the size of the as-formed nAgs (Yang *et al.*, 2003; Frattini *et al.*, 2005; Lee *et al.*, 2005; Son *et al.*, 2006). The absorption peak of nAg in the SF solutions containing $AgNO_3$ at 0.5, 1.0, 1.5, 2.0 and 2.5 wt.-% was first observed at 28, 22, 20, 20 and 17 h of aging time, respectively. The $AgNO_3$-containing SF solutions at 0.5 and 1.0 wt.-% exhibited the absorption peak of nAg at 413 - 456 nm, while the absorption band of $AgNO_3$-containing SF solutions at higher $AgNO_3$ concentrations (1.5, 2.0 and 2.5 wt.-%) showed slightly shift to 413-462 nm. At any given $AgNO_3$ content, the absorbance of the surface plasmon peak increased

with an increase in the aging period according to the increase in the number of the as-form nAg with an increase in aging period.

To study the effect of initial $AgNO_3$ concentration on the size of the as-prepared nAgs, the nAg-containing SF solutions that have been loaded with different $AgNO_3$ concentrations at the absorption intensity of 1.7 a.u. were selected and further casted into the nAg-loaded SF films. Fig. 2a shows the selected aging time (to obtain the intensity of surface plasmon absorption peak at 1.7 a.u.) and the average particle size of the as-prepared nAgs. The selected aging time for the preparation of the nAg-loaded SF films that had been prepared from the SF solutions containing the initial $AgNO_3$ about 0.5, 1.0, 1.5, 2.0 and 2.5 wt.-% was 36, 30, 26, 26 and 24 h, respectively. This result implied that the nAg in the $AgNO_3$-containing SF solutions that had been prepared from the SF solutions containing higher initial $AgNO_3$ concentrations occurred faster than those containing lower initial $AgNO_3$ concentrations. Furthermore, the relationship between the average size of the as-prepared nAg and the initial concentrations of $AgNO_3$ was observed. The size of the as-formed nAgs slightly increased with an increase in the initial $AgNO_3$ contents. The average size of Ag particles in the SF solutions containing $AgNO_3$ at 0.5, 1.0, 1.5, 2.0 and 2.5 wt.-% was about 8.71 ± 4.91, 9.96 ± 4.11, 11.50 ± 3.76, 11.77 ± 3.96 and 12.32 ± 3.76 nm, respectively as shown in Figure 6.2.

Figure 6.3 shows the morphology and the particle size distribution of nAgs formed in 2.5 wt.-% $AgNO_3$-containing SF solution. At any given $AgNO_3$ content, the as-formed nAgs displayed spherical shape and were distributed throughout the SF films. The well distribution of the as-formed particles within the film could possibly due to the complexation between nAgs and SF molecules.

Based on the results, it is obvious that the SF play a key role on the formation of nAgs in term of reduction and stabilization. SF is composed of about 15 amino acids, which glycine, serine, alanine and tyrosine are major amino acids of SF structure. Serine and tyrosine contain free hydroxyl functional groups that could be reduced silver ion to form silver metal or silver nanoparticle (Dong *et al.*, 2008). Furthermore the free carboxylic group of some amino acid residues such as aspartic and glutamic acid occurring in the amorphous polypeptide sequences (Arai *et al.*, 2001) were able to form complexes with metal cations. Therefore, SF acted as the

reducing agent that could reduce the silver ion to form silver metal or nAg in the SF solution and the stabilizing agent to prevent an agglomeration of the as-formed nAg.

6.4.2 Characterization of nAg-Loaded Gelatin Hydrogel Pads

6.4.2.1 In Vitro Degradation

In general, the SF film is water-soluble because it is fully amorphous, with its chains adopting a random-coil, rather than crystallization part. Here, methanol treatment was applied to induce a transition from random-coil to the β-sheet crystalline SF structure by dehydration (Gil *et al.*, 2007).

To assess their biodegradation, the nAg-loaded SF films were exposed to protease XIV enzyme (Horan, *et al.*, 2005), derived from *Streptomyces griseus*. Figure 6.4 shows the *in vitro* degradation of nAg-loaded SF films at initial $AgNO_3$ concentration of 2.5 wt.-% that had been submerged in simulated body fluid buffer solution (pH 7.4) with and without protease enzyme XIV at 37 °C. The nAg-loaded SF films after treatment with methanol contains highly ordered crystalline domains and less-ordered intermediate domains. For the SBF without protease, the nAg-loaded SF films still remained the weight of samples approximately 90 % over 260 h owning to methanol treatment. The degradation of the methanol-treated nAg-loaded SF film was negligible due to *β*-sheet conformation. For the SBF with protease, the weight loss of methanol-treated nAg-loaded SF films increased with an increase in submersion time. It can be concluded that SF is not self-degradable and can be degraded slowly in the presence of enzyme. This result corresponded with many finding (Li *et al.*, 2003; Arai *et al.*, 2004). The enzymatic degradation of methanol-treated nAg-loaded SF films could initially occur at amorphous regions and follow by *β*-sheet crystalline SF structure (Soong and Kenyon, 1984; Horan *et al.*, 2005).

6.4.2.2 Release Characteristics of Silver

The cumulative amount of silver released of the nAg-loaded SF films was determined by using AAS. Prior to investigating the characteristics of silver released from the nAg-loaded SF films, the actual amount of silver (either in the form of the free Ag^+ cations or the as-formed nAg) in these films needed to be determined. For this purpose, the methanol-untreated SF films that had been prepared from the SF solutions containing $AgNO_3$ at different concentrations (0.5, 1.0, 1.5, 2.0

and 2.5 wt.-%) were investigated the actual amount of silver by first dissolving in 95 % HNO_3, following by the addition of SBF. For the SF films that had been prepared from the SF solutions containing $AgNO_3$ at 0.75, 1.0, 1.5, 2.0 and 2.5 wt.-%, the theoretical contents of the as-loaded silver in these films should be 3.16, 6.29, 9.38, 12.45 and 15.49 mg/g of the films (in their dry state), respectively (or 63.19, 125.75, 187.69, 249.02 and 309.76 ppm/g of their dried films, respectively). Experimentally, the actual amounts of silver loaded at concentration of 0.5, 1.0, 1.5, 2.0 and 2.5 wt.-% in the films as determined by means of AAS in the SBF/HNO_3 solution were in ranges of 59.76 ± 11.70, 124.58 ± 25.10, 185.39 ± 8.06, 253.50 ± 23.27 and 304.89 ± 74.21 ppm/g of the films (n=3), respectively.

Figure 6.5 illustrates the cumulative amounts of silver, either in the form of nAgs or residual free ions (Ag^+), that were released per gram of the nAg-loaded SF films that had been loaded with varying amounts of $AgNO_3$ in SBF as a function of the submersion time. The release characteristics of silver from the films occurred in two stages. The first stage relates to the gradual release of silver from the films into the medium, which occurred within the first 72 h after submersion. At this time point, the cumulative amounts of silver released into the medium were 71.72 ± 6.33, 108.71 ± 2.93, 130.61 ± 20.32, 175.90 ± 21.50 and 166.85 ± 46.50 ppm/g of the films, which accounted to about 100, 76, 72, 73 and 50 % of the as-loaded amounts of silver within the films. The slow and sustain silver release could possibly due to the transformation of amorphous to β-sheet crystalline structure after methanol treatment. For second stage occurred between 72 h to 216 h, the cumulative amounts of silver in the medium leveled off to reach the final, maximum values of 71.72 ± 6.33, 143.49 ± 3.32, 180.40 ± 28.07, 242.06 ± 30.54 and 335.67 ± 78.45 ppm/g of the hydrogels. These values accounted to about 99 to 100% of the as-loaded amounts of silver within the films. Furthermore, at a given time, the result showed that increasing the $AgNO_3$ content increased the cumulative amounts of silver released in SBF.

6.4.2.3 Antimicrobial Activity

6.4.2.3.1 Antimicrobial Activity of $AgNO_3$ by MIC Determination

Minimum inhibitory concentration or MIC value was defined as the lowest concentrations giving no visible growth for each microorganism. The antimicrobial activities of the $AgNO_3$ were tested for seven strains such as *P. aeruginosa*, *S. aureus*, *S. aureus* (MRSA), *S. epidermidis*, *S. agalactiae*, *S. pyogenes* and *C. albicans*.

In general, *P. aeruginosa* typically infects the pulmonary tract, urinary tract, burns injuries, and also causes other blood infections. It is the most common cause of infections of wound and of the external ear. *S. aureus* can cause a range of illnesses from minor skin infections, such as pimple, impetigo, boil (furuncle), cellulitis, carbuncle, scalded skin syndrome, and abscess. *S. aureus* (MRSA) is especially troublesome in hospitals where patients with open wounds, invasive devices and weakened immune systems are at greater risk of infection than the general public. It is a bacterium responsible for several difficult-to-treat infections in humans. *S. epidermidis* is very likely to contaminate patient-care equipment and environmental surfaces and often occurs in people with weakened immune systems. It is a bacterium commonly present on human skin that sometimes causes human illness. This organism is typically resistant to multiple antibiotics and has become an important cause of serious infections in hospitalized patients. *S. agalactiae* is the major cause of bacterial septicemia of the newborn, which can lead to death. *S. pyogenes* is the cause of many important human diseases, ranging from mild superficial skin infections to life-threatening systemic diseases. *Candida albicans* is a diploid fungus (a form of yeast) and is most frequently infects the skin and mucosal surfaces.

The result shows that the MIC value of $AgNO_3$ against *S. aureus, P. aeruginosa*, *S. aureus* (MRSA), *S. epidermidis*, *S. agalactiae*, *S. pyogenes* and *C. albicans* was 2.4, 4.9, 4.9, 4.9, 4.9, 4.9 and 4.9 μg/ml, respectively as shown in Table 6.1. Based on the results, it can be concluded that $AgNO_3$ possessed strong antimicrobial activities for all of the tested microorganisms and had broad-spectrum antimicrobial properties. This behavior was also reported by Klasen, (2000).

6.4.2.3.2 Effects of The nAg containing Silk Fibroin Solutions on Microbial Growth

Figure 6.6 shows *In vitro* antimicrobial activity of the nAg containing SF solutions with various concentrations of $AgNO_3$ for microbial growth. As for the neat SF solution, the relative viability of all strain was equivalent to the control, a result that is in line with the nonbactericidal property. On the other hand, the nAg-containing SF solutions inhibited the growth of *C. albicans, P. aeruginosa* and *S. pyogenes* (Figure 6.6(g), (a) and (f)) more than *S. epidermidis, S. aureus, S. agalactiae* and *S. aureus* (MRSA) (Figure 6.6(d), (b), (e) and (c)) at any given concentration. Therefore, the nAg-containing SF solutions provided a broad spectrum of antimicrobial activity. Apparently, the increase in the antibacterial activity with an increase in the initial $AgNO_3$ concentration was due to the increased amounts of Ag^+ ions and the as-formed nAgs within the SF solution, which, in turn, were responsible for the increased amounts of the as released silver. With increasing time, the antibacterial activity was increased. Comparing the antibacterial activity between each stain, the nAg-loaded SF solution inhibited the growth of microbial stains in the following order: fungus *(C. albicans)* > Gram negative (*P. aeruginosa*) > Gram positive (*S. aureus, S. aureus* (MRSA), *S. epidermidis, S. agalactiae,* and *S. pyogenes*) bacteria.

6.4.2.3.3 Antimicrobial Disc Assay of The nAg-Loaded Silk Fibroin Films

In general, Ag ion selectively bind to thiol groups which are widely distributed in bacterial cell wall proteins, hence resulting in protein denaturation (Bechert *et al.*, 1999). The pathogens suffocate and die are cleared out of the body by the immune, lymphatic and elimination systems. Babu *et al.* (2006) reported that DNA loses its replication ability and cellular proteins become inactivated on silver ion treatment. Furthermore, Lee *et al.* (2005) proposed that when nAgs were present within the hydrogel membranes, the oxidation of Ag metal to Ag ions would occur to a greater extent at the surfaces of the nanoparticles. The Ag ions were the source of the antimicrobial activity.

Figure 6.7 shows the inhibition activity of the nAg-loaded SF films against *P. aeruginosa*. The inhibition zone or clear zone was the zone of no visible microbial colonies. It was found that no inhibition zone was

observed with the neat SF film whereas the nAg-loaded SF films exhibited the inhibition zone. The average inhibition zone including the sample diameter of the nAg-loaded SF films for all strains was summarized in Table 6.2. The average inhibition zone of the nAg-loaded SF films was found to increase with increasing the $AgNO_3$ contents. It means that the nAg-loaded SF films containing higher $AgNO_3$ contents could inhibit the growth of microorganisms more than those containing lower $AgNO_3$ contents. This result was consistent with the cumulative amount of Ag released. The nAg-containing SF films with higher $AgNO_3$ contents showed the higher cumulative amount of Ag released resulting in the greater inhibition zone. It should be noted that the nAg-loaded SF films inhibited the growth of microbial stains in the following order: fungus *(C. albicans)* > Gram negative (*P. aeruginosa*) > Gram positive (*S. aureus, S. aureus* (MRSA), *S. epidermidis, S. agalactiae* and *S. pyogenes*) bacteria. This result was substantiated by the antimicrobial activity of the nAg containing SF solutions (previous section). In addition, Taylor *et al.* (2005) also found that *P. aeruginosa* was more sensitive to the nanocrystalline silver than *S. aureus* as the % reduction for *P. aeruginosa* was higher than *S. aureus*. The weak effectiveness of the as-released silver against Gram-positive bacteria was postulated to be a result of thicker peptidoglycan layer within their cell wall, when compared with that of Gram-negative bacteria. The thick peptidoglycan layer within the cell wall of Gram-positive bacteria like *S. aureus* contains teichoic and lipoteichoic acids which act as chelating agents and could take part in the neutralization of the Ag^+ ions.

6.5 Conclusions

The nAg-loaded SF films were successfully prepared from a SF solution containing $AgNO_3$ with different concentrations. The formation of nAgs occurred through the in situ reduction with SF, which was also used as the stabilizing agent. The size of the as-formed nAgs was in the range 8-12 nm depending on the initial $AgNO_3$ contents. From *in vitro* degradation, the nAg-loaded SF films could be proteolytically degraded with an increase time of exposure to the enzyme. The total cumulative amount of silver released from the films that had been prepared from the

SF solutions containing higher initial $AgNO_3$ contents was greater than that containing lower initial $AgNO_3$ contents. The potential for use of the nAg-loaded SF films as wound dressings was assessed by antimicrobial activity against microorganism strains. The results showed that the nAg-loaded SF films inhibited the growth of microbial stains in the following order: fungus *(C. albicans)* > Gram negative (*P. aeruginosa*) > Gram positive (*S. aureus, S. aureus* (MRSA), *S. epidermidis, S. agalactiae,* and *S. pyogenes*) bacteria. Therefore, these nAg-loaded SF films could be possible used as antimicrobial wound dressings.

6.6 Acknowledgments

This project was supported in part by the National Nanotechnology Center (NANOTEC); the National Center of Excellence for Petroleum, Petrochemicals, and Advanced Materials (NCE-PPAM); the Petroleum and Petrochemical College (PPC), Chulalongkorn University; and Department of Biotechnology, Faculty of Science, Ramkhamhaeng University. VR acknowledges a doctoral scholarship received from the Thailand Graduate Institute of Science and Technology (TGIST) (TG-55-09-50-055D).

6.7 References

Alzoreky, N.S. and Nakahara, K. (2003) Antibacterial activity of extracts from some edible plants commonly consumed in Asia. International Journal Food Microbiology, 80(3), 223-230.

Altman, G.H., Horan, R.L., Lu, H.H., Moreau, J., Martin, I., Richmond, J.C., and Kaplan, D. L. (2002) Silk matrix for tissue engineered anterior cruciate ligaments. Biomaterials, 23(20), 4131-4141.

Altman, G.H., Diaz, F., Jakuba, C., Calabro, T., Horan, R.L., Chen, J., Lu, H., Richmond, J., and Kaplan, D.L. (2003) Silk-based materials. Biomaterials, 24(3), 401-416.

Arai, T., Freddi, G., Colonna, G.M., Scotti, E., Boschi, A., Murakami, R., and Tsukada, M. (2001) Absorption of metal cations by modified *B. mori* silk

and preparation of fabrics with antimicrobial activity. Journal of Applied Polymer Science, 80(2), 297-303.

Arai, T., Freddi, G, Innocenti, R., and Tsukada, M. (2004) Biodegradation of *Bombyx mori* silk fibroin fibers and films. Journal of Applied Polymer Science, 91(4), 2383-2390.

Babu, R., Zhang, J., Beckman, E.J., Virji, M., Pasculle, W.A., and Wells, A. (2006) Antimicrobial activities of silver used as a polymerization catalyst for a wound-healing matrix. Biomaterials, 27(24), 4304-4314.

Barry, A.L. (1976) Agar dilution techniques, Lea and Febiger, Philadelphia, (pp. 76-104).

Bauer, A.W., Kirby, W.M.M., Sherris, J.C., and Turck, M. (1966) Antibiotic susceptibility testing by a standardized single disk method. American Journal of Clinical Pathology, 36, 493-496.

Bechert, T., Boswald, M., Lugauer, S., Regenfus, A., Greil, J., and Guggenbichler, J.P. (1999) The Erlanger silver catheter: in vitro results for antimicrobial activity. Infection, 27, 24–29.

Chirila, T.V., Barnard Z., Harkin, D.G., Schwab, I.R., & Hirst, L.W. (2008).Bombyx mori silk fibroin membranes as potential substrate for epithelial constructs used in the management of ocular surface disorders. Tissue Engineering Part A, 14(7), 1203-1211.

Chou, K. S. and Lai, Y.S. (2004) Effect of polyvinyl pyrrolidone molecular weights on the formation of nanosized silver colloids. Materials Chemistry and Physics, 83(1), 82-88.

Dong, Q., Su, H., Cao, W., Han, J., Zhang, D., and Guo, Q. (2008) Biogenic synthesis of hierarchical hybrid nanocomposites and patterning of silver nanoparticles. Materials Chemistry and Physics, 110(1), 160-165.

Field, C.K. and Kerstein, M.D. (1994) Overview of wound healing in a moist environment. The American Journal of Surgery, 167(1A), S2-S6.

Frattini, A., Pellegri, N., Nicastro, D., and de Sanctis, O. (2005) Effect of amine groups in the synthesis of Ag nanoparticles using aminosilane. Materials Chemistry and Physics, 94(1), 148-152.

Gallant-Behm, C.L., Yin, H.Q., Liu, S., Heggers, J.P., Langford, R.E., Olson, M.E., Hart, D.A., and Burrell, R.E. (2005) Comparison of in vitro disc diffusion and time kill-kinetic assays for the evaluation of antimicrobial wound dressing efficacy. Wound Repair and Regeneration, 13(4), 412–421.

Gamo, T., Inokuchi, T., and Laufer, H. (1977) Polypeptides of fibroin and sericin secreted from the different sections of the silk gland in *Bombyx mori*. Insect Biochemistry, 7(3), 285-295.

Gil, E.S., Frankowski, D.J., Hudson, S.M., and Spontak, R.J. (2007) Silk fibroin membranes from solvent-crystallized silk fibroin/gelatin blends: Effects of blend and solvent composition. Materials Science and Engineering C, 27(3), 426-431.

Hanawa, T., Watanabe, A., Tsuchiya, T., Ikoma, R., Hidaka, M., and Sugihara, M. (1995) New oral dosage form for elderly patients: preparation and characterization of silk fibroin gel. Chemical and Pharmaceutical Bulletin, 43(2), 284-288.

Hardy, J.G. and Scheibel, T.R. (2010) Composite materials based on silk proteins. Progress in Polymer Science, 35(9), 1093–1115.

Horan, R.L., Antle, K., Collette, A.L., Wang, Y., Huang, J., Moreau, J.E., Volloch, V., Kaplan, D.L., and Altman, G.H. (2005) *In vitro* degradation of silk fibroin. Biomaterials, 26(17), 3385-3393.

Huang, L.M., Tsai, C.C., Wen, T.C., and Gopalan, A. (2006) Simultaneous synthesis of silver nanoparticles and poly(2,5-dimethoxyaniline) in poly(styrene sulfonic acid). Journal of Polymer Science: Part A: Polymer Chemistry, 44(12), 3843-3852.

Jones, S.A., Bowler, P.G., Walker, M., and Parsons, D. (2004) Controlling wound bioburden with a novel silver-containing Hydrofiber dressing. Wound Repair and Regeneration, 12(3), 288–294.

Khanna, P.K., Singh, N., Charan, S., Subbarao, V.S., Gokhale, R., and Mulik, U.P. (2005) Synthesis and characterization of Ag/PVA nanocomposite by chemical reduction method. Materials Chemistry and Physics, 93(1), 117-121.

Kim, K.D., Han, D.N., and Kim, H.T. (2004) Optimization of experimental conditions based on the Taguchi robust design for the formation of nanosized silver particles by chemical reduction method. Chemical Engineering Journal, 104(1-3), 55-61.

Klasen, H.J. (2000) Historical review of the use of silver in the treatment of burns I. Early uses. Burns, 26(2), 117-130.

Li, M., Ogiso, M., and Minoura, N. (2003) Enzymatic degradation behavior of porous silk fibroin sheets. Biomaterials, 24(2), 357-365.

Lin, F., Li, Y.C., Jin, J., Cai, Y.R., Wei, K.M., and Yao, J.M. (2008) Deposition behavior and properties of silk fibroin scaffolds soaked in simulated body fluid. Materials Chemistry and Physics, 111(1), 92-97.

Leaper, D.J. (2006) Silver dressings: their role in wound management. International Wound Journal, 3(4), 282–294.

Lee, D., Cohen, R.E., and Rubner, M.F. (2005) Antibacterial properties of Ag nanoparticle loaded multilayers and formation of magnetically directed antibacterial microparticles. Langmuir, 21(21), 9651-9659.

Lee, H.K., Jeong, E.H., Baek, C.K., and Youk, J.H. (2005) One-step preparation of ultrafine poly(acrylonitrile) fibers containing silver nanoparticles. Materials Letters, 59(23), 2977-2980.

Lee W.F. and Tsao, K.T. (2006) Preparation and properties of nanocomposite hydrogels containing silver nanoparticles by ex situ polymerization. Journal of Applied Polymer Science, 100(5), 3653-3661.

Minoura, N., Tsukada, M., and Nagura, M. (1990) Physico-chemical properties of silk fibroin membrane as a biomaterial. Biomaterials, 11(6), 430-434.

Minoura, N., Tsukada, M., and Nagura, M. (1990) Fine structure and oxygen permeability of silk fibroin membrane treated with methanol. Polymer, 31(2), 265-269.

National Committee for Clinical Laboratory Standards. (1990) Approved standard M7-A2. Standard methods for dilution antimicrobial tests with bacteria that grow aerobically, 2nd edn. Villanova, PA, National Committee for Clinical Laboratory Standards (pp 30-89).

Qiu, X.Q., Wang, H., Lu, X.F., Zhang, J., Li, S.F., Cheng, G., Wan, L., Yang, L. Zuo, J.Y., Zhou, Y.Q., Wang, H.Y., Cheng, X., Zhang, S.H., Ou, Z.R., Zhong, Z.C., Cheng, J.Q., Li, Y.P., *and* Wu, G.Y. (2003) An engineered multidomain bactericidal peptide as a model for targeted antibiotics against specific bacteria. Nature Biotechnology, 21, 1480-1485.

Rattanaruengsrikul, V., Pimpha, N., and Supaphol, P. (2009) Development of gelatin hydrogel pads as antibacterial wound dressings. Macromolecular Bioscience, 9(10), 1004-1015.

Sondi, L., Goia, D.V., and Matijevic, E. (2003) Preparation of highly concentrated stable dispersions of uniform silver nanoparticles. Journal of Colloid Interface Science, 260(1), 75-81.

Soong, H.K. and Kenyon, K.R. (1984) Adverse reactions to virgin silk sutures in cataract surgery. Ophthalmology, 91(5), 479-483.

Taylor, P.L., Ussher, A.L., and Burrell, R.E. (2005) Impact of heat on nanocrystalline silver dressings: Part I: Chemical and biological properties. Biomaterials, 26, 7221-7229.

Takasu, Y., Hiromi, Y., and Kozo, T. (2002) Isolation of three main sericin components from the cocoon of the silkwarm, *Bombyx mori*. Bioscience Biotechnology and Biochemistry, 66(12), 2715-2718.

Uchida, M. (1995) Antimicrobial zeolite and its application. Chemical Industrial, 46(5), 48-54.

Velikov, K.P., Zegers, G.E., and Vanblaaderen, A. (2003) Synthesis and characterization of large colloidal silver particles. Langmuir, 19(4), 1384-1389.

Wright, J.B., Lam, K., Buret, A.G., Olson, M.E., and Burrell, R.E. (2002) Early healing events in a porcine model of contaminated wounds: effects of nanocrystalline silver on matrix metalloproteinases, cell apoptosis, and healing. Wound Repair and Regeneration, 10(3), 141–151.

Wuand, C. and Tian, B. (1996) Third International Silk Conference, Suzhou.

Yang, Q.B., Li, D.M., Hong, Y.L., Li, Z.Y., Wang, C., Qiu, S.L., and Wei, Y. (2003) Preparation and characterization of a PAN nanofiber containing Ag nanoparticles via electrospinning. Synthetic Metals, 137(1-3), 973-974.

Table 6.1 Minimum inhibition concentration of $AgNO_3$ against microorganism strains

Microorganisms	Minimum inhibition concentration (μg/ml)
1. *Pseudomonas aeruginosa* (ATCC 27853)	> 4.9
2. *Staphylococcus aureus* (ATCC 25923)	> 2.4
3. *Staphylococcus aureus* (MRSA) (DMST 20654)	> 4.9
4. *Staphylococcus epidermidis* (ATCC 12228)	> 4.9
5. *Streptococcus agalactiae* (DMST 17129)	> 4.9
6. *Streptococcus pyogenes* (DMST 17020)	> 4.9
7. *Candida albicans* (ATCC 10231)	> 4.9

Note; ATCC: American Type Culture Collection

DMST: Department of Medical Sciences

Table 6.2 Average lengths of the inhibition zones (including the diameter of sample) of the neat SF films and the nAg-loaded SF films that had been incubated at 37 °C for 24 h against microorganisms

Microorganisms	Diameter of inhibition zone (cm)				
	0.5%$AgNO_3$	1.0%$AgNO_3$	1.5%$AgNO_3$	2.0%$AgNO_3$	2.5%$AgNO_3$
1. *P. aeruginosa*	1.72	1.82	1.90	1.99	2.02
2. *S. aureus*	1.65	1.81	1.93	1.96	1.94
3. *S. aureus* (MRSA)	1.50	1.50	1.50	1.67	1.67
4. *S. epidermidis*	1.65	1.77	1.95	1.92	1.99
5. *S. agalactiae*	1.69	1.75	1.81	1.84	1.86
6. *S. pyogenes*	1.81	1.84	1.89	1.98	2.00
7. *C. albicans*	1.85	2.14	2.07	2.25	2.26

Note; Diameter of sample: 1.5 cm

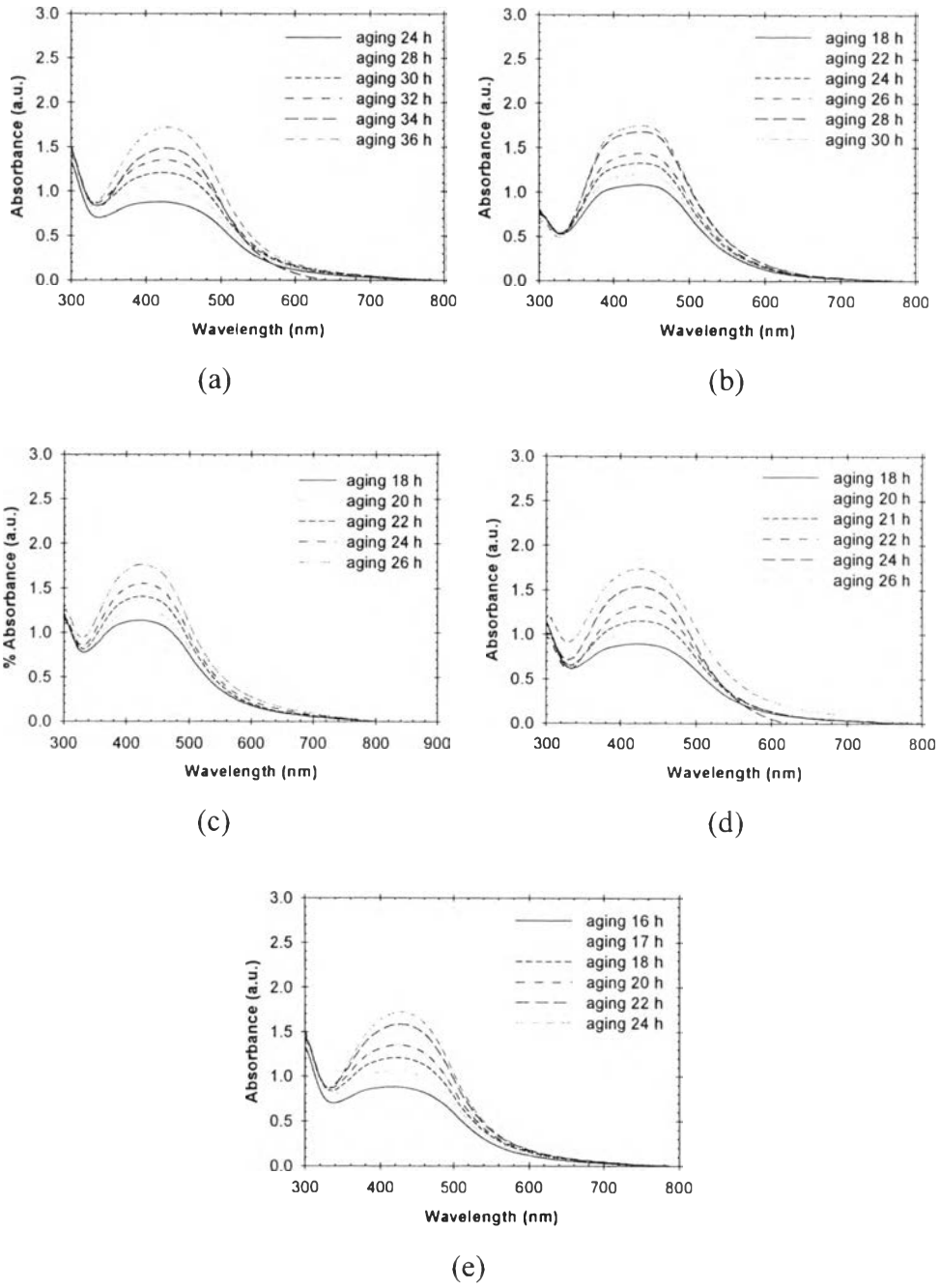

Figure 6.1 shows UV-visible absorption spectra of the $AgNO_3$-containing SF solutions that had been aged for various time intervals with different $AgNO_3$ contents (a) $AgNO_3$ 0.5 wt.-%, (b) $AgNO_3$ 1.0 wt.-%, (c) $AgNO_3$ 1.5 wt.-%, (d) $AgNO_3$ 2.0 wt.-% and (e) $AgNO_3$ 2.5 wt.-%. The pink text is the chosen aging time for further fabrication to films.

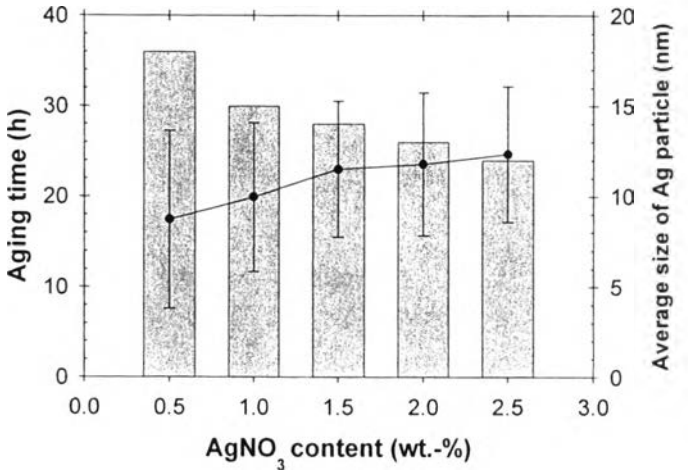

Figure 6.2 shows the selected aging time of the nAg containing SF solutions (for left Y-axis) and the average size of Ag particle (for right Y-axis) with different concentrations of $AgNO_3$ 0.5, 1.0, 1.5, 2.0 and 2.5 wt.-%.

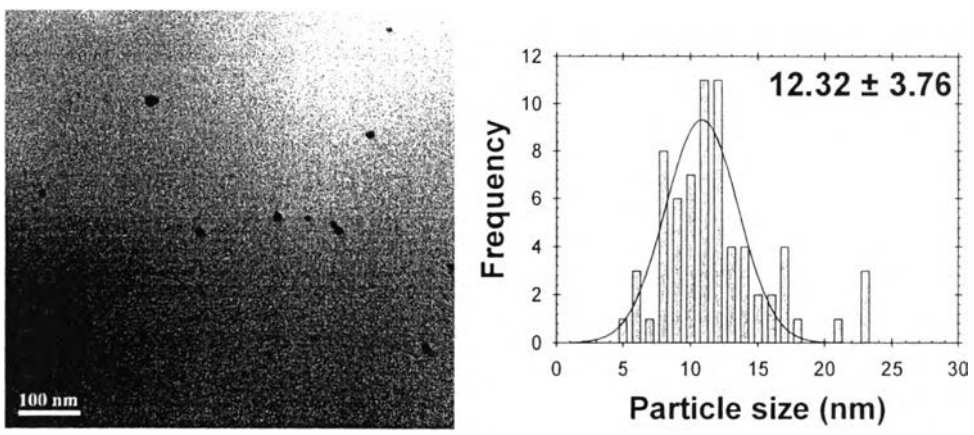

Figure 6.3 Selected TEM image and histogram (magnification = 20,000x; scale bar = 100 nm) of silver nanoparticles (nAgs) formed in 2.5 wt.-% $AgNO_3$-containing SF solution that had been aged for 24 h.

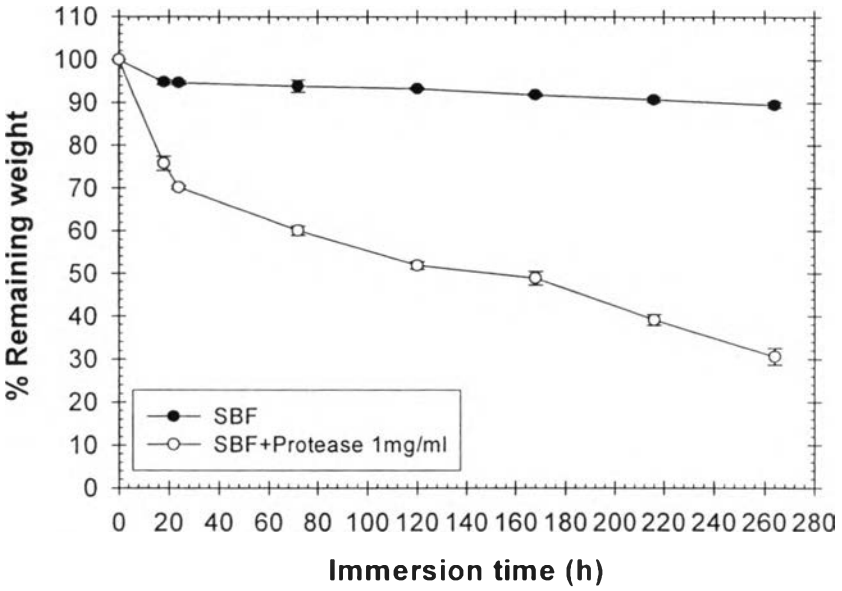

Figure 6.4 *In vitro* degradation of nAg (2.5 wt.-% $AgNO_3$) loaded SF films that had been submerged in SBF with and without Protease enzyme XIV at 37 °C (n=3).

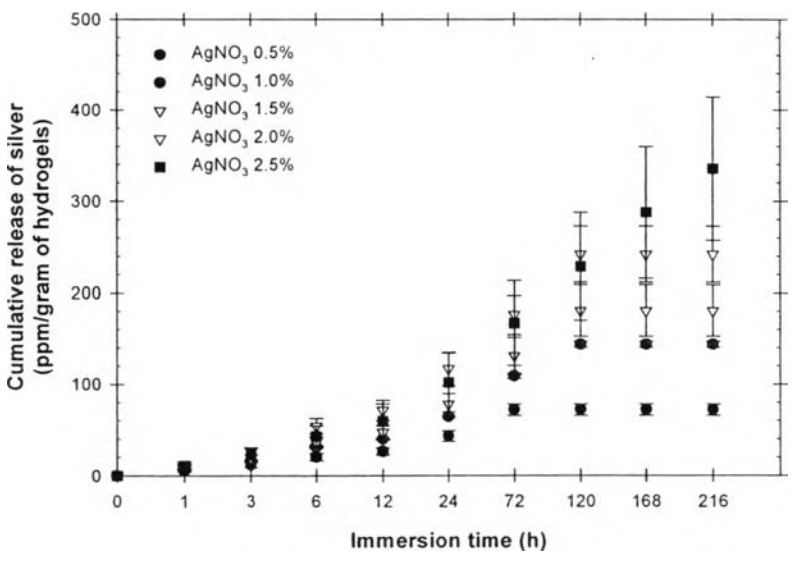

Figure 6.5 Cumulative release of silver from the nAg-loaded SF films that had been submerged in SBF solution (pH 7.4) at 37 °C for various time intervals (n = 3). Different data sets were for the films that had been loaded with different $AgNO_3$ contents.

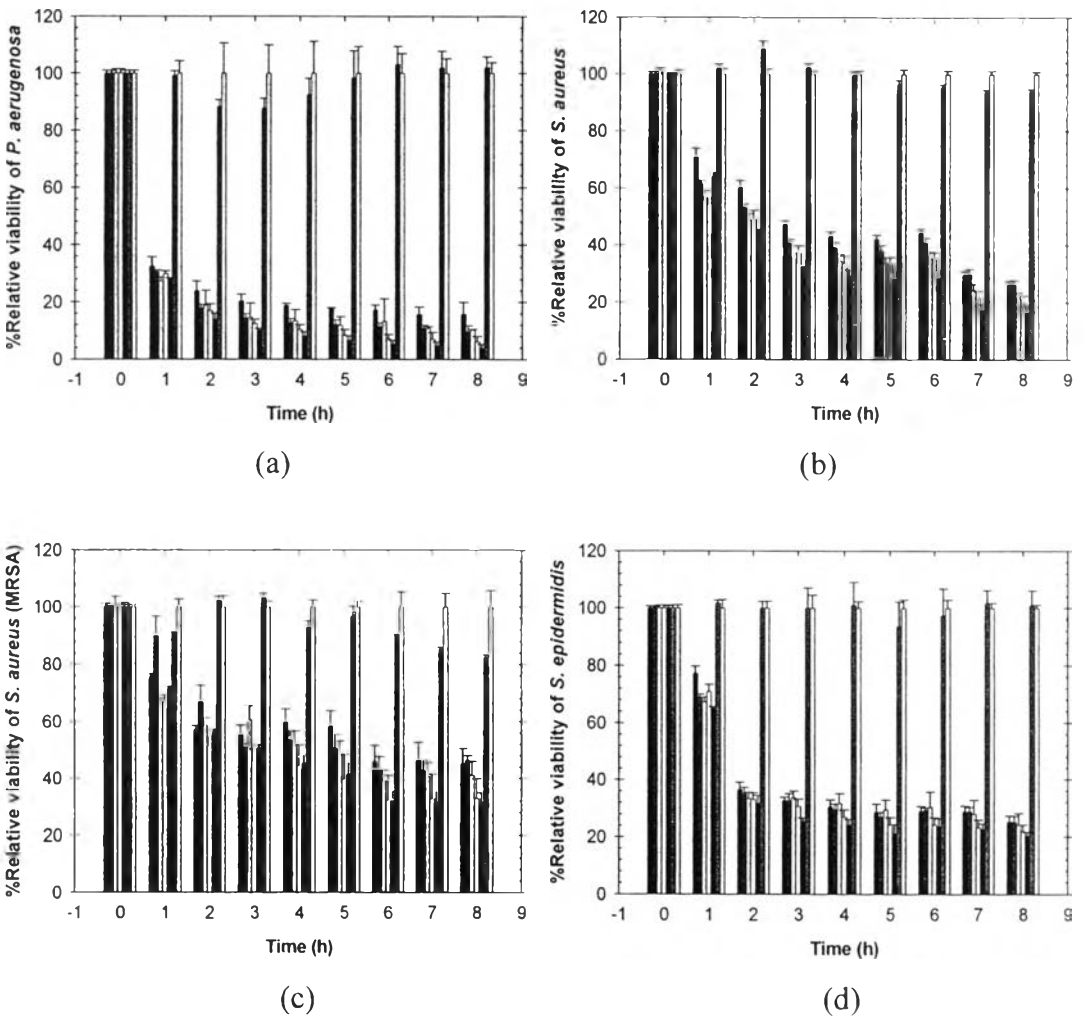

Figure 6.6 *In vitro* antimicrobial activity of the nAg containing SF solutions with various concentrations of $AgNO_3$ for microbial growth. (a) *P. aeruginosa,* (b) *S. aureus,* (c) *S. aureus* (MRSA), (d) *S. epidermidis,* (e) *S. agalactiae*, (f) *S. pyogenes* and (g) *C. albicans*. Different data sets were • the control, • the neat SF solution and the nAg-containing SF solutions that had been prepared from different initial $AgNO_3$ contents: • 0.5, •1.0, • 1.5, • 2.0 and • 2.5%.

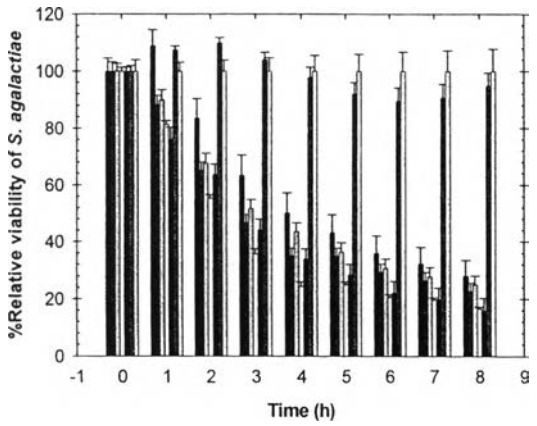

(e)

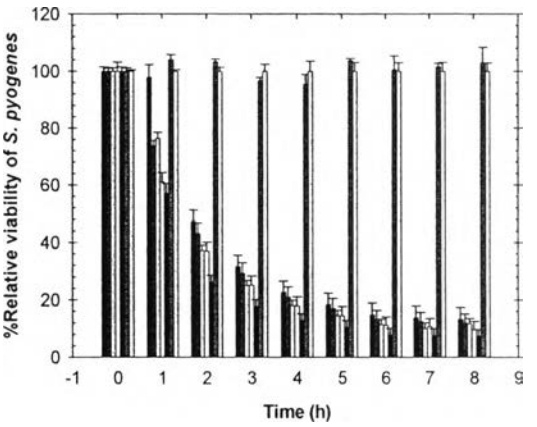

(f)

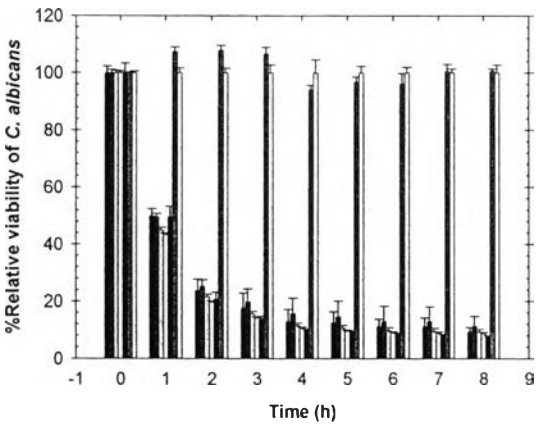

(g)

Figure 6.6 (continued).

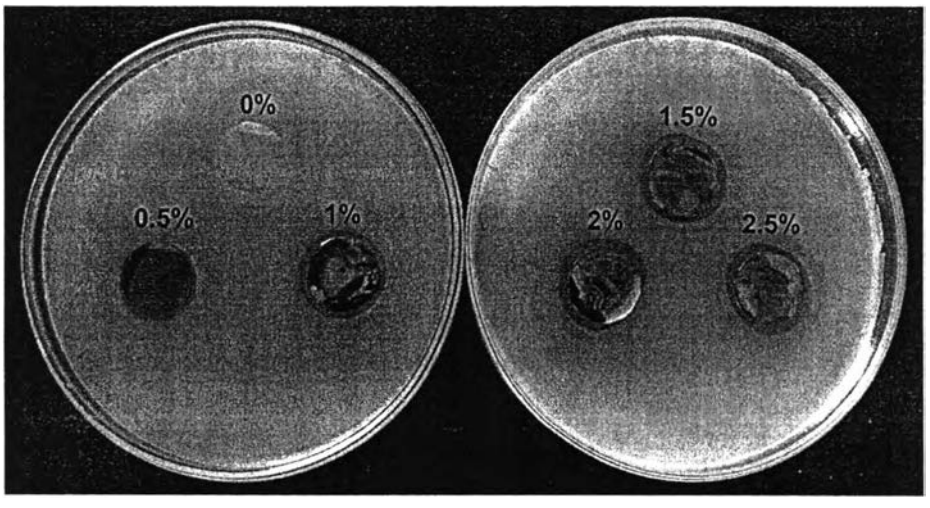

Figure 6.7 Illustration of the inhibition zone of the nAg-loaded SF films with containing in various $AgNO_3$ contents. The neat SF film was used as the control. The films were tested against with *P. aeruginosa* and incubated at 37 ^{o}C for 24 h.